

1 **Fecal bacteria contamination of floodwaters and a coastal waterway from tidally-**
2 **driven stormwater network inundation**

3 **M. M. Carr¹, A. C. Gold², A. Harris³, K. Anarde³, M. Hino⁴, N. Sauers¹, G. Da Silva¹, C.**
4 **Gamewell¹, and N. G. Nelson^{3,5}**

5 ¹Department of Biological and Agricultural Engineering, North Carolina State University,
6 Raleigh, NC.

7 ²Environmental Defense Fund, Raleigh, NC.

8 ³Department of Civil, Construction, and Environmental Engineering, North Carolina State
9 University, Raleigh, NC.

10 ⁴Department of City and Regional Planning, University of North Carolina - Chapel Hill, Chapel
11 Hill, NC.

12 ⁵Center for Geospatial Analytics, North Carolina State University, Raleigh, NC.

13 Corresponding author: Natalie Nelson (nnelson4@ncsu.edu)

14 **Key Points:**

- 15 • Daily observations of *Enterococcus spp.* concentrations in a coastal waterway were
16 similar during and outside perigean spring tides.
- 17 • Tidal inundation of stormwater networks occurred daily, but rainfall runoff produced the
18 greatest bacterial contamination in the waterway.
- 19 • High *Enterococcus spp.* concentrations were observed in roadway floodwaters and the
20 receiving waterway during perigean spring tides.

21 Abstract

22 Inundation of coastal stormwater networks by tides is widespread due to sea-level rise (SLR).
23 The water quality risks posed by tidal water rising up through stormwater infrastructure (pipes
24 and catch basins), out onto roadways, and back out to receiving water bodies is poorly
25 understood but may be substantial given that stormwater networks are a known source of fecal
26 contamination. In this study, we (1) documented temporal variation in concentrations of
27 *Enterococcus spp.* (ENT), the fecal indicator bacteria standard for marine waters, in a coastal
28 waterway over a two-month period and more intensively during two perigean spring tide periods,
29 (2) measured ENT concentrations in roadway floodwaters during tidal floods, and (3) explained
30 variation in ENT concentrations as a function of tidal inundation, antecedent rainfall, and
31 stormwater infrastructure using a pipe network inundation model and robust linear mixed effect
32 models. We find that ENT concentrations in the receiving water body vary as a function of tidal
33 stage and antecedent rainfall, but also site-specific characteristics of the stormwater network that
34 drains to the waterbody. Tidal variables significantly explain measured ENT variance in the
35 waterway, however, runoff drove higher ENT concentrations in the receiving waterway. Samples
36 of floodwaters on roadways during both perigean spring tide events were limited, but all samples
37 exceed thresholds for safe public use of recreational water. These results indicate that inundation
38 of stormwater networks by tides could pose public health hazards in receiving water bodies and
39 on roadways, which will likely be exacerbated in the future due to continued SLR.

40 Plain Language Summary

41 Communities along the US Atlantic Coast have begun to experience the effects of sea-level rise
42 as stormwater drainage pipes, originally designed when sea levels were lower, are now routinely
43 inundated at high tide. We do not know whether frequent inundation of stormwater drainage
44 pipes affects coastal water quality, specifically the fecal bacteria levels of coastal waters. In this
45 study, we collected daily measurements of *Enterococcus spp.* (ENT), the bacteria used by
46 regulators to assess the safety of marine waters for swimmers and recreators, from a tidal creek
47 over a two-month period. We also collected water samples during the highest high tides from
48 roadway floodwaters and the adjacent tidal creek as the stormwater pipes drained during the
49 outgoing tide. After data collection, we developed statistical models to relate the amount of ENT
50 in the tidal creek to tide, rainfall, and stormwater infrastructure. When comparing rainfall and
51 tide, we observed that rainfall caused greater bacterial contamination in the tidal creek than high
52 tide flooding. However, we observed high ENT concentrations in roadway floodwaters and in
53 the creek during the outgoing tide, leading us to conclude that everyday flooding of underground
54 stormwater pipes at high tide could create hazardous water quality.

56 1 Introduction

57 Since 1880, global sea level has risen between 21 and 24 cm due to the melting of land-
58 based ice and thermal expansion of ocean water (Sweet et al., 2022). On the United States' South
59 Atlantic and Gulf coasts, sea levels locally have risen at even higher rates (approximately 10 mm
60 year⁻¹) due to internal climate variability (e.g., increased wind-driven ocean circulation) and local
61 land elevation changes (i.e., subsidence and isostatic rebound) (Dangendorf et al., 2023).

62 This accelerated rate of local (relative) sea-level rise (SLR) poses a threat to coastal
63 communities, many which were built on low-lying land. Specifically, for many of these coastal

64 communities, stormwater infrastructure, like subterranean pipe networks, ditches, and catch
65 basins, was built decades ago when sea levels were lower. Increased water levels have allowed
66 tides to propagate up into stormwater networks and overtop low elevation areas, causing coastal
67 communities to flood in what is referred to as "sunny day flooding" or "high tide flooding".
68 Regular tidal inundation of stormwater networks has become widespread in coastal areas (Gold
69 et al., 2022), and persistent increases in SLR are projected to increase the frequency and
70 magnitude of high tide flooding nationally (Sweet et al., 2022).

71 As tidal floods increase in frequency and magnitude, aging and faulty stormwater
72 infrastructure may pose a public health risk by creating water quality hazards (Allen et al., 2019).
73 Stormwater networks can act as reservoirs for fecal contaminants, as exfiltrated sewage (Hart et
74 al., 2020; Olds et al., 2018), biofilms (Burkhart, 2013), or septic leachate (Converse et al., 2011)
75 can be present within the network. Frequent inundation by tidal waters could transport fecal
76 contaminants from stormwater networks to roadways during incoming or flood tides, and flush
77 pollutants into coastal waters during outgoing or ebb tides. Other factors, like stormwater runoff
78 (Shen et al., 2019; Gold et al., 2023) and high groundwater tables (Befus et al., 2023; Habel et
79 al., 2020), can compound with tides and reduce the volume capacity of stormwater networks,
80 leading to more extensive or frequent flooding of coastal communities.

81 In coastal waters, fecal contamination is often measured by *Enterococcus spp.* (ENT)
82 concentrations. ENT are gram-positive cocci bacteria typically found in the intestines of warm-
83 blooded mammals. Because of their origin in intestines, ENT are used as a fecal indicator
84 organism in marine and beach water quality standards from the U.S. Environmental Protection
85 Agency (EPA, Recreational Water Quality Criteria, 2012). ENT concentration is a proxy
86 measure for gastrointestinal illness risk in marine waters (Wade et al., 2021).

87 Increased attention has been dedicated to tidal inundation as a transport mechanism of
88 fecal contamination through stormwater infrastructure inundation (Hart et al., 2020; Price et al.,
89 2021), overtopping of coastal infrastructure (Macías-Tapia et al., 2021, 2023), and groundwater
90 inundation (McKenzie et al., 2021). Hart et al. (2020) measured human-specific microbial source
91 tracking markers in a municipal separate stormwater system (MS4) in Beaufort, NC, during
92 compound high tide and storm conditions, proposing that diluted sewage could be present in
93 standing water on the roadway when high tide floods occur. This work was continued by Price et
94 al. (2021), who determined that the highest concentrations of fecal indicator bacteria (FIB),
95 including ENT, in stormwater discharge were present in receding tides during nineteen sampling
96 events encompassing both storm and ambient conditions. Macías-Tapia et al. (2021, 2023)
97 reported consistent exceedances of ENT in tidal floodwaters of the Lafayette River in Norfolk,
98 VA, during five annual perigean spring tide flooding events between 2017 and 2021. Perigean
99 spring tides occur during the coincidence of perigee – when the moon is closest to the Earth in its
100 orbit and therefore exerts a large gravitational pull resulting in higher than average tides – and
101 spring tide (during a new or full moon, when the Earth, moon, and sun are in alignment).
102 Because perigean spring tides produce some of the highest water levels of the year, they can
103 result in coastal flooding of low-lying areas. The work of Macías-Tapia et al. (2021, 2023)
104 determined that in Norfolk, loads varied between perigean spring tide floods but no relationship
105 between ENT abundance and floodwater extent could be determined (Macías-Tapia et al., 2023).
106 Lastly, McKenzie et al. (2021) monitored coastal and canal groundwater and surface water and
107 storm drains during high tide events and reported the presence of wastewater discharge in the
108 collected samples through measurement of radon and wastewater tracers. Combined, these

109 studies provide insight into the potential role of tidal flooding as a mechanism for fecal
110 contamination in coastal waters. However, to understand how stormwater network inundation by
111 tides is a driver of coastal fecal contamination, longitudinal data are needed to understand how
112 contaminant dynamics vary across locations, over time, and with flood events of different drivers
113 (e.g., tides and rainfall) and magnitudes.

114 In this study, we assessed the potential for fecal contamination in an urban, coastal
115 waterway that experiences tidal floods and daily inundation of its underground stormwater
116 network by tides. Specifically, our objectives were to (1) document temporal variation in fecal
117 bacteria concentrations in a coastal waterway over multiple flood events and under baseline
118 conditions, (2) measure fecal bacteria concentrations in roadway floodwaters during tidal flood
119 events, and (3) explain variation in bacteria concentrations as a function of tidal inundation,
120 antecedent rainfall, and stormwater infrastructure. Since fecal contaminants are highly variable
121 in space and time (Boehm, 2007), we collected observational data at three locations daily over a
122 two month period, and more intensively during nine tidal cycles coinciding with two perigean
123 spring tide events (i.e., some of the highest tide events of the year, when the moon is closest to
124 the earth). These measurements, in conjunction with a simplified pipe network model and linear
125 regression, were used to explain variation in bacteria concentrations in the waterway as a
126 function of tidal inundation, antecedent rainfall, and stormwater infrastructure.

127 **2 Methods**

128 2.1 Site Description

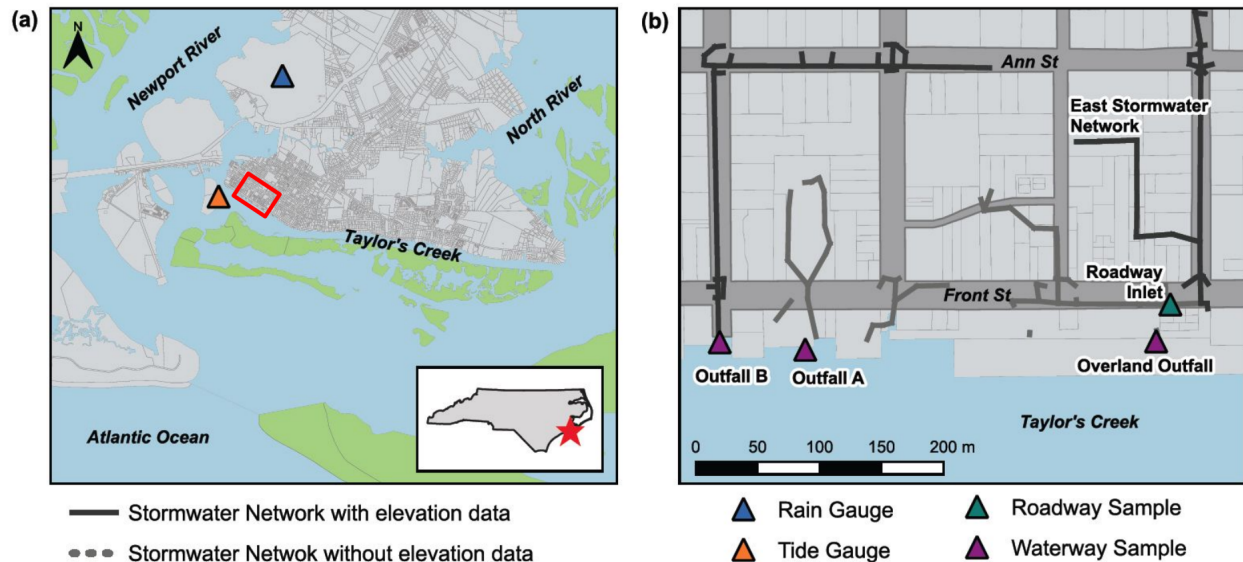
129 Our study site was Beaufort, North Carolina, USA, a small, coastal town established in
130 the 1700s. Beaufort sits on a peninsula between the Newport River and North River (to the west
131 and east, respectively) and north of Taylor's Creek, a tidal channel that empties through an inlet
132 to the Atlantic Ocean. We focused our sampling efforts on Taylor's Creek, which is the receiving
133 waterbody that is adjacent to the downtown area, and on the roadway closest to the waterway
134 Front Street (**Fig 1a**). The tides in Taylor's Creek are semi-diurnal with a tidal range of 0.95 m
135 (NOAA Tides and Currents Station ID: 8656483, located in Beaufort, NC). In 2016, Taylor's
136 Creek was listed as a 303(d) impaired waterway for ENT by the North Carolina Division of
137 Environmental Quality, but was later delisted in 2022 after stormwater network improvements
138 (NCDEQ, 2022 North Carolina 303(d) List, 2023).

139 Much of the shoreline in the downtown area is armored with bulkheads, which protects
140 roadways and other low-lying areas from high water levels in Taylor's Creek. Stormwater is
141 conveyed to Taylor's Creek via a MS4, consisting of subterranean pipes and several outfalls
142 within our sampling area (**Fig 1b**). Roadway flooding is monitored on Front Street by water level
143 gauges located within the stormwater network, as well as pole-mounted cameras (Gold et al.,
144 2023). These data have shown that tides inundate the stormwater network on a daily basis;
145 during perigean spring tide events, water can rise all the way up through the network and result
146 in flooding of roadways. During regular tides, flooding can still occur due to the compounding
147 effects of rainfall, as there is limited capacity for pipes to convey even small amounts of rainfall
148 as a result of tidal water volumes occupying some of the capacity (Gold et al., 2023).

149 Two spring tides (here, full moons) coinciding with a moon orbit in perigee occurred
150 during the study period on June 14 and July 13, 2023 (NOAA, 2022). During the highest-high
151 tides associated with these perigean spring tide events, tidal waters propagated up through the

152 stormwater network and produced minor roadway flooding nine times. No concomitant rainfall
 153 occurred during the highest-high tides of the two perigean spring tide events, so that the
 154 floodwaters were produced from tidal influence only. Rainfall occurred during the higher low
 155 tide on July 15, 2022, and produced a compound flood event (i.e., rainfall coincided with tidal
 156 inundation).

157



158

159 **Figure 1.** Study map of Beaufort, NC (USA) with an inset map showing the location of Beaufort
 160 within North Carolina as a red star (a) and the four stormwater networks in the study area (b). In
 161 (a), the red rectangle indicates the study area. The green land area represents natural areas, the
 162 gray land area represents developed areas, and the thin gray lines delineate land parcels. The
 163 NOAA tide gauge (orange triangle), which informed sampling times and provided data for tidal
 164 variables, is located across Taylor's Creek approximately 300 m from the Outfall B sampling
 165 location. The rain gauge (blue triangle) is located north of the study site. In (b), thick gray lines
 166 show the underground stormwater pipe network, with the shade of gray indicating whether there
 167 was elevation data available (dark and light for networks with known and unknown elevation,
 168 respectively). Waterway samples were collected from Taylor's Creek at three locations (purple
 169 triangles) within 2 meters of stormwater network outfalls. Roadway flood samples were
 170 collected directly above a single stormwater catchment grate in the East network (teal triangle).

171 2.2 Data Collection

172 Water quality samples were collected for enumeration of ENT concentrations, which is a
 173 proxy measure for fecal contamination. Collection occurred at three waterway locations in
 174 Taylor's Creek (**Fig 1b**). The "Overland Outfall" sampling location is near a bulkhead spillway
 175 that conveys stormwater runoff from a parking lot and is not connected to the subterranean pipe
 176 network. The overland outfall is relatively high in elevation and was not observed to be
 177 inundated during our study period. The "Outfall A" drains a relatively small area (**Fig 1b**),
 178 including a parking lot around a museum and catch basins on Front Street. The "Outfall B"
 179 sampling location drains a relatively large area, including a residential street and catch basins on
 180 Front Street and Ann Street (**Fig 1b**). The Outfall B sampling location was added on June 14,
 181 2022, a week after sampling was initiated at the Overland Outfall and the Outfall A locations.

182 Outfall elevations were only available for the Outfall B, which is positioned at -0.74 m NAVD88
183 or -0.30 m Mean Higher-High Water (MHHW). The MHHW datum is the mean of the highest
184 diurnal tide, and is useful for identifying extremes in tidal heights. Water levels greater than the 0
185 m MHHW datum are deviations of tidal heights above the average high tide. At this elevation,
186 the Outfall B is inundated by tides on a daily basis.

187 Collection of water samples in Taylor's Creek, proximate to the three outfall locations
188 described above, occurred daily for 58 days from June 6 to August 2, 2022. This allowed for
189 characterization of fecal contamination during both baseline conditions and perigean spring tides.
190 Baseline sampling of ENT occurred daily between 8:00-9:00 AM Eastern Time to prevent ENT
191 levels from being affected by UV inactivation from direct sunlight, which peaks around midday.
192 Given the two-month long sampling period, the daily samples also captured every tidal stage
193 (low, rising, high, falling tide). Perigean spring tide sampling of ENT occurred on June 12-16
194 and July 11-15, 2022, when estimated water levels were above the local risk-based threshold.
195 During these high water level events, we increased the sampling frequency to include
196 measurements at high tide, ebb tide (approximately halfway between high and low tide), and low
197 tide, with measurement times scheduled based on predicted water levels at the nearby NOAA
198 Tides and Currents Station (NOAA, ID 8656483; Fig 1). This sampling frequency was selected
199 to capture the change in fecal contamination conditions from the maximum stormwater
200 inundation (at highest high tide) and during the draining of the stormwater networks (during the
201 ebb tide and at the highest low tide). During these floods, we also sampled roadway floodwaters
202 at a stormwater grate in the easternmost stormwater network of the downtown area, referred to as
203 the "East" network (n = 10). We define a roadway flood as any amount of water above the
204 elevation of the stormwater grate. In total, 166 samples were collected from Taylor's Creek
205 under baseline conditions (58 at Overland Outfall and Outfall A, 50 at Outfall B) and 89 during
206 perigean spring tide events (30 at Overland Outfall and Outfall A and 29 at Outfall B,
207 corresponding to 3 measurements per studied tidal cycle, with five cycles being measured in
208 each of the two perigean spring tide periods). Additionally, 10 samples were collected from
209 roadway floodwaters (9 tidal floods, 1 compound flood).

210 Sterile, pre-rinsed 100 mL FalconTubes (polypropylene material) attached to a sampling
211 pole were used to collect 100 mL water samples from Taylor's Creek at 0.5-1 m below the water
212 surface across three locations that were within 2 meters of stormwater network outfalls. For
213 flood water samples collected at the roadway inlet, collection occurred by hand at water surface
214 depth. After collection, samples were stored in a cooler at 4°C during transport to the laboratory.
215 Water samples were processed in duplicate for ENT following the IDEXX Enterolert standard
216 protocol with the Quanti-tray 2000 (IDEXX, ASTM Method #D6503-99). The IDEXX assay
217 requires a 100 mL sample volume. Per the IDEXX Enterolert protocol, due to the brackish
218 salinities of the water samples, 10 mL of water sample was mixed with 90 mL of deionized water
219 during processing. Samples were provided the IDEXX media and incubated for 24 hours at 41°C
220 ± 0.5°C. ENT concentrations were estimated using a most-probable number (MPN) technique
221 based on the number of large and small wells of the quanti-trays fluorescing under UV light,
222 with a modified laboratory detection range of 10-24,196 most probable number ENT per 100 mL
223 water (MPN 100 mL⁻¹) due to sample dilution. During sample collection and laboratory analysis,
224 field blanks (n = 27) and laboratory blanks (n = 30) were also collected and processed for quality
225 assurance and quality control purposes. Field blanks consisted of deionized water in sample
226 bottles that were transported to and from the field in a sample cooler, and opened and recapped at

227 one or more of the sampling sites. Lab blanks consisted of deionized water in sample bottles that
228 remained in the lab and were not transported to the field.

229 ENT concentrations were classified as above or below the EPA's single sample
230 maximum threshold concentration for safe public use of recreational waters of 104 MPN 100
231 mL⁻¹ (EPA, Recreational Water Quality Criteria, 2012). This EPA standard is for recreational use
232 of marine waters, meaning it directly applies to water samples collected from Taylor's Creek, but
233 does not directly apply to the assessment of roadway floodwaters, which are not recreational
234 waters. Given that a standard does not exist for floodwaters of any kind – whether storm or
235 tidally driven – but that pedestrians can still make contact with floodwaters, we consider the
236 EPA's recreational standard here as a benchmark for comparison of water quality measurements
237 collected from the roadway during the tidal floods.

238 2.3 Pipe Network Inundation Model

239 A pipe network inundation model of Front Street was used to characterize the extent of
240 tidal inundation within the stormwater network during the measured flood events. Generally, a
241 pipe network inundation model is a “bathtub” approach that simulates flooding by gradually
242 filling subterranean pipes based on the elevation of the pipe relative to tidal stage (Strauss et al.,
243 2012). The pipe network inundation model used in this study was generated using the *bathtub* R
244 package (Gold et al., 2022) and is the same model used by Gold et al. (2022) for Beaufort, NC.
245 This model was developed using elevations from a 2017 survey, during which some structures
246 were inaccessible. Hence, our pipe network inundation model is incomplete for the Front Street
247 study area, but can be used to estimate stormwater network inundation in two of the studied
248 stormwater pipe systems, specifically the pipe networks of the Outfall B and Roadway Inlet
249 (located in the East network) sampling locations (**Fig 1b**). The percentage of stormwater network
250 inundation was quantified at discrete water levels by averaging the percent fill of surveyed
251 stormwater point structures (e.g., drop inlets and catch basins) on Front Street.

252 2.4 Explanatory Variables used in Linear Regressions

253 We sought to explain measured variation in ENT concentrations within the waterway
254 with both tidal and rainfall factors using robust linear mixed effect regressions of the baseline
255 sampling and the perigeon spring tide sampling data. Tidal variables used in the explanatory
256 analysis include tidal height at time of sample collection, time since the last high tide before
257 sample collection, and the height of the last high tide before sample collection. Tidal height at
258 the time of sample collection was taken from the nearby NOAA Tides and Currents gauge (Fig
259 1a, which has been shown to match well with measured water levels in a stormwater catch basin
260 on Front Street when it is not raining (Gold et al., 2023). The height of the last high tide, and the
261 time since the last high tide, were likewise calculated using the NOAA tide gauge data. We
262 chose to include time since the last high tide before sample collection and the height of the last
263 high tide before sample collection to account for a potential lagged response of ENT
264 concentrations in the waterway as tidal waters recede from the stormwater network, relative to
265 the timing of maximum inundation of the stormwater network. While additional meteorological
266 observations are available at the NOAA tide gauge, such as air temperature, we chose to only
267 focus on the effects of tide and rain given our study period spanned two summer months and,
268 thus, was not long enough to account for the effects of seasonal variation.

269 Because Taylor’s Creek is a coastal waterway, it receives ENT loads by both direct
270 runoff from stormwater outfalls and fluvial transport through the local watershed. To account for
271 these transport pathways, we considered rainfall factors in the explanatory analysis. Seven
272 rainfall variables were analyzed, all of which correspond to (antecedent) rainfall totals over finite
273 intervals, including rainfall over 3, 6, 12, 24, 36, 48, and 72 hours prior to sample collection (in
274 mm). These variables were calculated using hourly rainfall depths (millimeters) obtained from
275 the Michael J Smith Airport weather station located approximately a mile north of Front Street in
276 Beaufort, NC (North Carolina State Climate Office, station ID: KMRH; **Fig 1a**). The June
277 rainfall total was 50 mm, and only one storm event produced a rainfall depth over 13 mm (or
278 0.51 inches). In contrast, the July rainfall total was 400 mm and 8 storm events produced rainfall
279 depths greater than 13 mm.

280 2.5 Regression Analysis

281 ENT concentrations from the waterway were first logarithmically transformed to account
282 for the exponential range of bacteria counts observed. The relationship between logarithmically
283 transformed ENT concentrations (\log_{10} ENT) and sampling location was then assessed using the
284 Friedman test, which is a hypothesis test for repeated measures. We selected the Friedman test
285 because the daily collection of ENT constitutes a repeated measure and the test does not assume
286 an underlying distribution for the grouped-by-location data. The Friedman test determines
287 whether the median value of a treatment group is significantly different from the median values
288 of the other treatment groups. We assessed significance with an alpha value of 0.05. The
289 Friedman test was calculated using the *stats* R package (R Core Team, 2013).

290 Next, the relationships between \log_{10} ENT, tidal, and rainfall variables were analyzed
291 using two sets of robust linear mixed effect models with the *robustlmm* R package (Koller,
292 2016). We selected robust linear mixed effect models because of the repeated-measures structure
293 of our sampling design and the presence of outliers and non-normal residuals in the \log_{10} ENT
294 data set. The first set of models (the “baseline” models) used data from the entire two-month
295 study period, which captured daily stormwater network inundation and multiple rain events. The
296 second set of models (the “perigean spring tide” models) used data only from the perigean spring
297 tide sampling that corresponded with complete inundation of the stormwater network and
298 roadway flooding (i.e., the nine roadway flood events spanning June 12-16 and July 11-15,
299 2022). Data collected during baseline sampling and perigean spring tide sampling were modeled
300 separately due to differences in sampling design, and to allow for assessment of relationships
301 between tide and rainfall variables under distinct conditions. The model sets were comprised of
302 individual robust linear mixed effect regressions between \log_{10} ENT and a single explanatory
303 variable to evaluate pairwise relationships.

304 Given that the waterway data varies both in space and time, the baseline mixed effect
305 model has the following equation structure:

$$\log_{10} \text{ ENT} = \text{Explanatory Variable} + (1 \mid \text{Site}) \quad \text{Equation 1}$$

306 Where “|” denotes that the sampling location, or “Site”, is a random effect. The perigean spring
307 tide model has the equation structure:

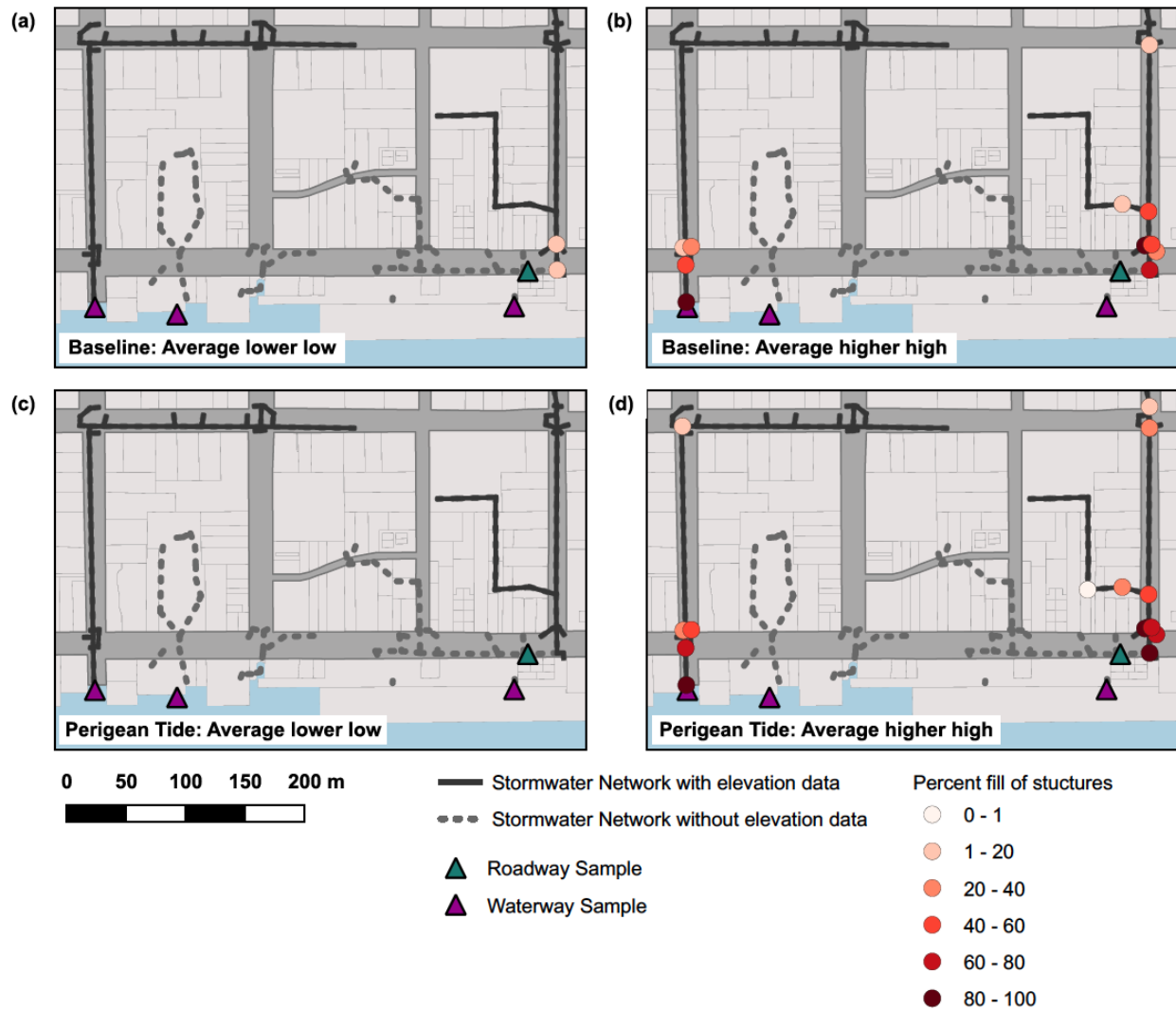
$$\log_{10} \text{ ENT} = \text{Explanatory Variable} + (1 \mid \text{Site}) \\ + (1 \mid \text{Perigean Spring Tide} / \text{Categorical Tidal Stage}) \quad \text{Equation 2}$$

308 Where “Site” and “Perigean Spring Tide” (June or July) are random effects and “Categorical
309 Tidal Stage” (high, ebb, and low tide) is a nested random effect within the “Perigean Spring
310 Tide” random effect. No interaction exists between the “Site” and “Perigean Spring Tide /
311 Categorical Tidal Stage” terms because the sampling design produced a crossed-data structure
312 between sampling period and site. The tidal and rainfall explanatory variables are fixed effects
313 and were centered and scaled in the baseline models and perigean spring tide models.
314 Conditional R^2 (variance explained by random and fixed effects) and marginal R^2 (variance
315 explained by fixed effects or explanatory variables) were calculated for each regression using the
316 *performance* R package (Lüdtke et al., 2021). Results are discussed in terms of their marginal
317 R^2 value since marginal R^2 values only include the effect of the explanatory variable while
318 conditional R^2 values also include the effects of random variables. Additionally, p-values and
319 slopes were calculated to identify significant positive or negative relationships ($\alpha = 0.05$)
320 using the *parameters* R package (Lüdtke et al., 2020). All analyses were performed using R
321 version 4.2.2 (R Core Team, 2022).

322 **3 Results and Discussion**

323 3.1 Tidal stormwater network inundation occurred daily

324 Water level data from within a storm drain on Front Street showed that the East network
325 was inundated daily over the two month study period at each higher-high tide ($n = 58$, Gold et
326 al., 2023). Using the pipe network model, we find that the stormwater network along other areas
327 of Front Street was on average 57% inundated during the higher-high tides (on average 0.16 m
328 MHHW) and 0.6% inundated during the lower-low tides (on average -0.91 m MHHW) during
329 baseline conditions (**Fig 2a-2b**). During the perigean spring tide events, the average lower low
330 tide and higher high tide elevations were -1.1 and 0.40 m MHHW, respectively, which
331 correspond to modeled stormwater network inundation percentages of 0 and 78% along Front
332 Street, respectively (Fig 2c-2d). During these events, inundation of the stormwater network
333 extended inland beyond Front Street, filling pipes nearly 40% with tidal water (**Fig 2c**).



334
 335 **Figure 2.** Modeled tidal inundation of two stormwater networks in downtown Beaufort during
 336 the study period. The average percent fill of stormwater catchments (attached to subterranean
 337 pipes) is shown for lower low tide (2a,c) and higher high tide (2b,d) for the baseline data
 338 collected from June 6 to August 2, 2022 (2a,b), and for the perigean spring tide data collected on
 339 June 12-17 and July 11-16, 2022 (2c,d).

340 Our pipe network model only accounts for variation in tidal elevation, as measured by the
 341 nearby NOAA tide gauge, and does not consider water level contributions from rainfall runoff,
 342 groundwater infiltration into the stormwater network, or pipe hydraulics. Bathtub models, like
 343 the pipe network model used here, typically overestimate flooding compared to models that
 344 account for pipe hydraulics (e.g., Castrucci & Tahvildari, 2018; Gallien et al., 2014). However,
 345 outside of rain events, Gold et al. (2023) showed that water levels in the East network track well
 346 with water levels measured at the NOAA tides gauge during baseline conditions, indicating that
 347 contributions from groundwater infiltration into the stormwater network are likely small for the
 348 pipe network. During rainfall events, the pipe network model is an underestimate of actual
 349 inundation.

350 While the network inundation model does not consider non-tidal forcing and pipe
351 hydraulics, it can be used to estimate where inundation was relatively high and low across the
352 network due to tidal forcing alone. In particular, the network inundation estimates highlight that
353 total network inundation and roadway flooding were most likely to occur in and along the East
354 network. The pipe network model also reveals that the Outfall B network experienced daily and
355 major inundation, but to a lesser extent than the East network. Due to the inlet and outfall
356 elevations not being surveyed, we are unable to assess the frequency at which the Outfall A
357 network was inundated.

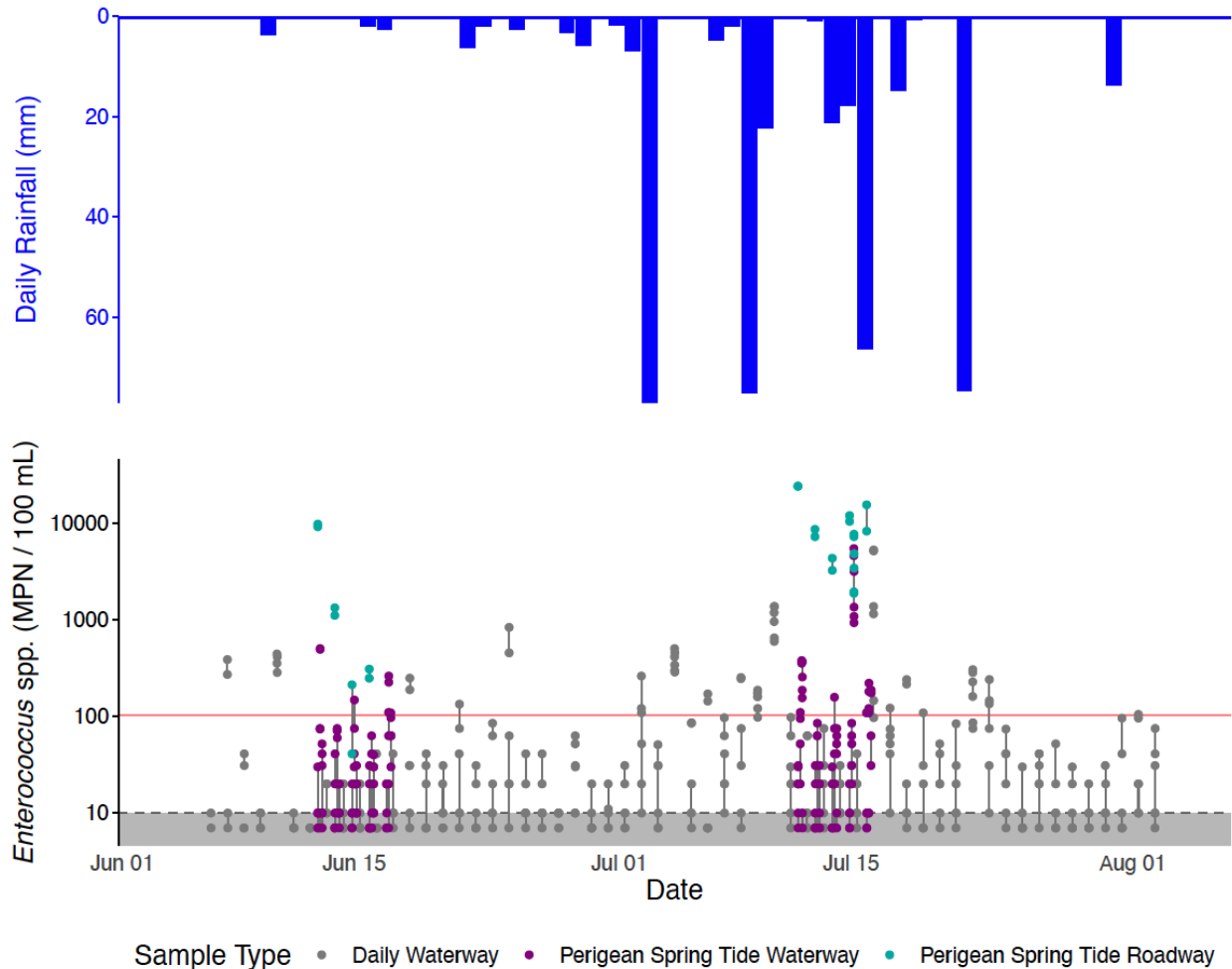
358 3.2 Daily waterway ENT concentrations differed between sampling locations

359 ENT was detected in 73% of daily, or baseline, samples ($n = 241/330$) with
360 concentrations ranging from 10 to 5,298 MPN 100 mL⁻¹ (**Fig 3**). ENT measurements exceeded
361 the single sample maximum threshold concentration for safe public use of recreational waters
362 (104 MPN 100 mL⁻¹) in 16% of the daily samples, indicating recurring but infrequent levels of
363 unsafe fecal contamination in the waterway during the two month summer sampling period.
364 Similar daily ENT concentrations in the waterway were observed between non-perigean and
365 perigean spring tide periods. Hence, while perigean spring tide events lead to increased
366 stormwater network inundation (**Fig 2d**), they did not necessarily result in increased ENT
367 loading within the waterway.

368 We also found there were significant differences in ENT concentrations by sampling
369 location (p -value = 0.004, **Table S1**). During baseline conditions, Outfall B had the highest
370 median concentration of ENT in the waterway (31 MPN 100 mL⁻¹) while the sampling locations
371 near Outfall A and Overland Outfall showed lower median ENT concentrations (both 10 MPN
372 100 mL⁻¹, which corresponds to the minimum detection limit). Inter-site variability between
373 outfall sampling locations was also noted by Price et al. (2021), who posited that site-specific
374 infrastructure can cause localized water quality dynamics. However, while significant differences
375 were observed across sites, the median concentrations demonstrate how ENT levels were
376 frequently low, and well below the EPA recreational water quality standard.

377 In addition to varying by location, median ENT concentrations across all outfall locations
378 differed between the months of June and July 2022 (**Fig 3, Table S2**). For June, the median ENT
379 concentration was 20 MPN 100 mL⁻¹ and had an interquartile range of <10 to 23 MPN 100 mL⁻¹
380 while the July median concentration was 41 MPN 100 mL⁻¹ and had an interquartile range of 10
381 to 86 MPN 100 mL⁻¹. Rainfall occurred more frequently in July than in June. Periods of
382 increased rainfall are known to correspond with increased FIB concentrations in waterways due

383 to runoff-driven contamination and elevated surficial groundwater elevations, which can also
384 lead to greater sewage exfiltration (Secru et al., 2011).



385
386 **Figure 3.** Daily rainfall (top) and ENT concentrations (bottom) during flood (perigean spring
387 tide) and baseline conditions throughout June and July 2022. ENT concentrations are plotted on
388 a log₁₀ scale. The red line represents the EPA's single sample maximum threshold concentration
389 for safe public use (104 MPN 100 mL⁻¹), and the grayed area represents the minimum detection
390 limit (below 10 MPN 100 mL⁻¹ for samples diluted 10:1). Gray and purple points correspond to
391 measurements taken in Taylor's Creek during baseline and flood conditions at the three sampling
392 locations, respectively, while teal points correspond to measurements taken from roadway
393 floodwaters above a single stormwater catchment grate in the East network. Samples were
394 processed in duplicate, and duplicate measurements are connected by vertical lines to visualize
395 uncertainty.

396 3.3 Roadway floodwaters had consistently high ENT concentrations

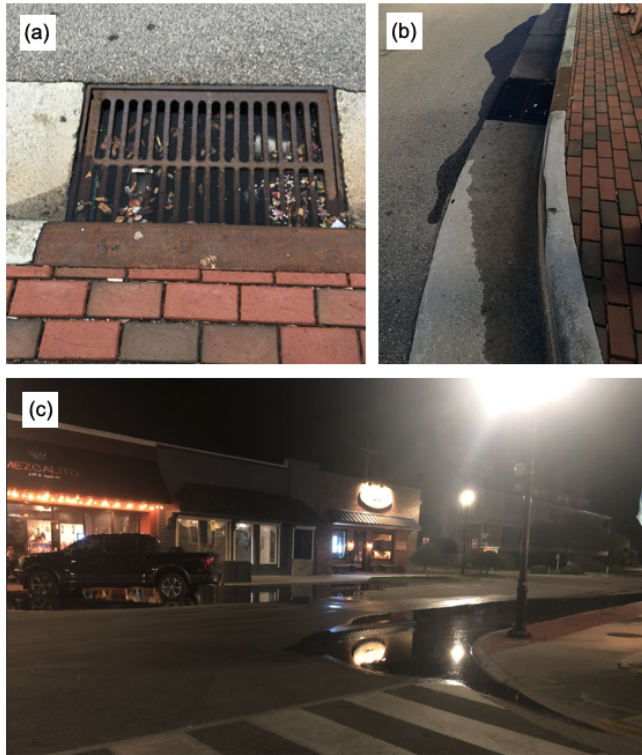
397 We visually observed nine minor floods localized to the East stormwater network, and no
398 roadway flooding via the Outfall A and Outfall B stormwater networks during perigean spring
399 tides. The presence of flooding was corroborated by the storm drain water level measurements
400 and the pipe network model. The floodwater samples exceeded the EPA's single sample

401 maximum threshold concentration for safe public use (104 MPN 100 mL⁻¹) for 8 of the 9 high
402 tide flood events, in many cases by an order of magnitude (**Fig 3**). These ENT concentrations are
403 comparable to the concentrations reported by Macías-Tapia et al. (2021, 2023) in Norfolk, VA in
404 2017, when 95% of the ENT samples exceeded the single sample maximum threshold
405 concentration and ENT concentrations ranged from 30 to >24,000 MPN 100 mL⁻¹.

406 In June, the median floodwater concentration was 710 MPN 100 mL⁻¹ and concentrations
407 ranged from 41 to 9,804 MPN 100 mL⁻¹ (**Fig 3**). By comparison, in July, the median floodwater
408 concentration was 9,563 MPN 100 mL⁻¹ and concentrations ranged from 1,882 to >24,196 MPN
409 100 mL⁻¹. The perigean high tide elevations were similar between June and July (0.35-0.51 and
410 0.34-0.45 m MHHW, respectively), as was the modeled inundation percentages at higher high
411 tide (75-87 and 73-81%), so we hypothesize that differences in concentrations stem from
412 antecedent rainfall factors. These findings suggest that antecedent rainfall can enhance fecal
413 contamination in roadway floodwaters during high tide flood events. But, importantly, given that
414 the June floodwaters were still more than 6 times higher than the EPA standard in the absence of
415 rainfall, complete inundation of stormwater networks by tides in drier conditions can create
416 concerning water quality conditions in roadway floodwaters.

417 The sources of fecal bacteria in the roadway floodwater samples are unknown. We
418 believe the primary fecal bacteria sources during the high tide floods sampled were within the
419 stormwater network. We observed fecal contamination in roadway floodwaters in the absence of
420 rain, due solely to stormwater network inundation by tides, indicating a source from either
421 Taylor's Creek or the stormwater network. However, water quality samples collected near
422 stormwater outfalls in Taylor's Creek did not have similarly high concentrations (**Fig 3**), so
423 Taylor's Creek is likely not a primary source of fecal bacteria to the floodwaters. Lastly, the
424 majority of the roadway floods were small and confined to puddles around the storm drains (**Fig**
425 **4**), indicating that the floodwaters likely did not flush fecal matter from the land surface.

426 Because tidal inundation of stormwater networks can impede drainage of stormwater
427 runoff, it may be that stormwater runoff with high ENT concentrations remain in the network as
428 stagnant water for extended periods of time, potentially spilling into the roadway during the next
429 high tide. Additional sources of fecal bacteria in the stormwater network could include
430 exfiltrated sewage (Hart et al., 2020), and local environmental reservoirs of bacteria in biofilms
431 and sediment (Burkhart, 2013). Importantly, since the majority of our measurements were
432 collected from roadway floods with small overland extents, we are unable to assess whether high
433 ENT concentrations would persist during more extensive floods, or if more extensive floods may
434 dilute ENT concentrations instead, as proposed by Lewis et al. (2013).



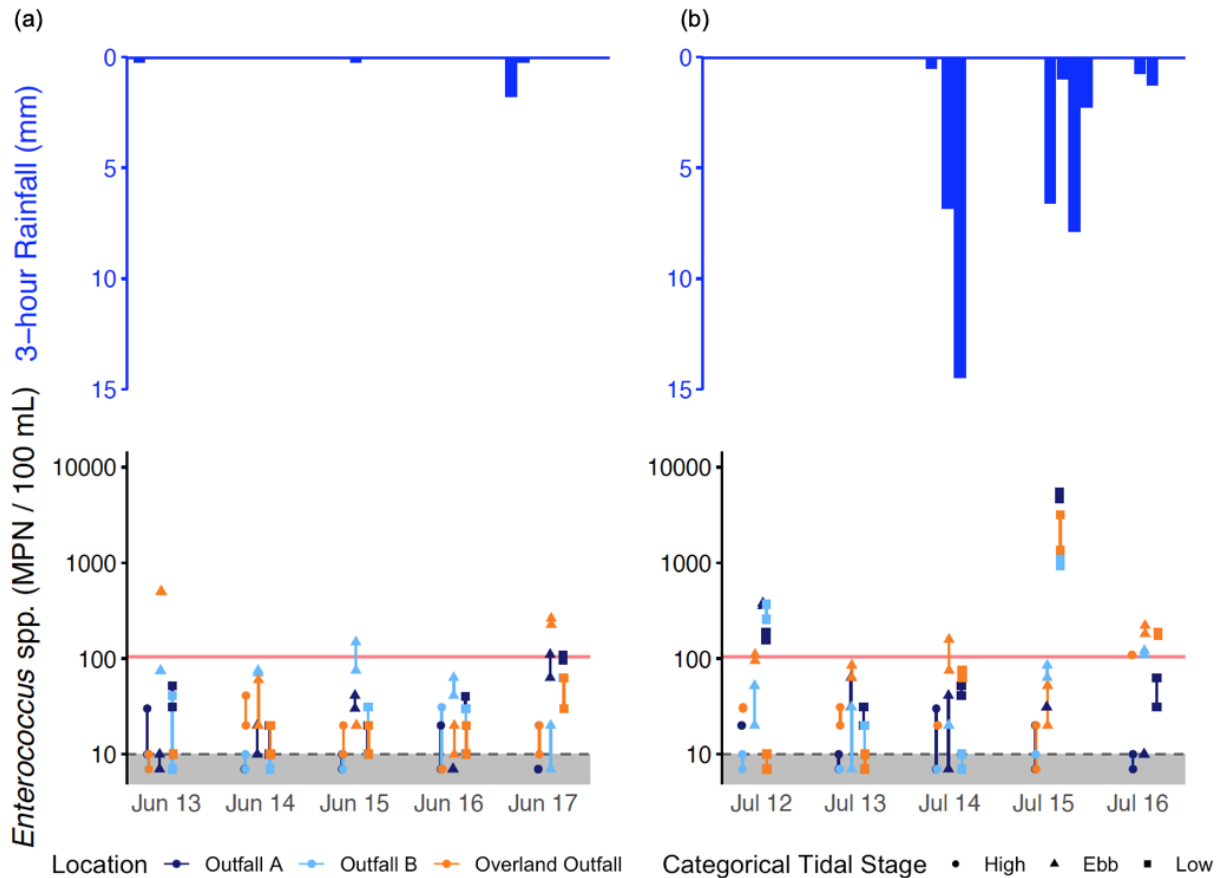
435

436 **Figure 4.** Tidal flooding at high tide on June 12, 2022 at 7:18PM (a), June 14, 2022 at 8:52PM
437 (b), and June 15, 2022 at 9:51PM (c). We define a roadway flood as any amount of water above
438 the elevation of the stormwater grate.

439 3.4 Highest median ENT concentrations occurred during ebb tide

440 To capture the water quality of receding tidal waters from the stormwater network during
441 the perigeon spring tide events, ENT measurements were collected at multiple tidal stages in the
442 waterway: at high tide, ebb tide, and low tide (**Fig 5**). We observed a general trend that ENT
443 concentrations increased from high tide to ebb tide and decreased from ebb tide to low tide. This
444 trend has been previously reported for Taylor’s Creek in Price et al. (2021), who observed that
445 ENT increased during ebb tide as tidal height decreased and the stormwater network drained. In
446 this present study, median concentrations at high, ebb, and low tide across both the June and July
447 perigeon spring tide events were 10, 52, and 30.5 MPN 100 mL⁻¹, respectively (**Fig 5**). Sixty
448 percent (n = 36/60) of high tide samples had ENT concentrations below the minimum detection
449 limit of 10 MPN 100 mL⁻¹. Then, as the tidal waters receded from the stormwater network during
450 ebb tide, ENT concentrations increased, with exceedances of the EPA recreational water quality
451 standard primarily occurring on ebb tide. From the linear regression analysis, we found that this
452 trend was reflected in a significant negative relationship (coefficient = -0.28, p-value < 0.001)
453 between tidal stage at sample collection and ENT concentrations in the perigeon spring tide
454 models (Table 1). This increase in median ENT concentrations from high to ebb tide suggests
455 that receding tides transport ENT from the stormwater network to the waterway. However, we
456 also observe a decrease in median ENT concentrations from ebb to low tide, which suggests that
457 the effect of receded tidal waters on ENT concentrations in the waterway was short lived. This
458 could potentially be explained by flushing or dilution. UV inactivation should not have affected

459 the measured ENT concentrations given that the perigean spring tide sampling occurred at night
 460 during both the June and July events. While most of the EPA recreational water quality standard
 461 exceedances occurred from samples collected during ebb tide, a few exceedances were observed
 462 outside of ebb tide during the last monitored tidal cycle, which occurred following rainfall (**Fig**
 463 **5b**).



464
 465 **Figure 5.** 3-hour rainfall (top) and ENT concentrations (bottom) from Taylor's Creek during
 466 perigean spring tide events from June 12-17, 2022 (a) and July 11-16, 2022 (b). The red line
 467 represents the EPA's single sample maximum threshold concentration for safe public use (104
 468 MPN 100 mL⁻¹), and the grayed area represents the minimum detection limit (below 10 MPN
 469 100 mL⁻¹ for samples diluted 10:1). Point shapes correspond to the tidal stages of high, ebb, and
 470 low, while the colors correspond to sampling locations.

471 Although the highest ENT concentrations in the waterway during the perigean spring tide
 472 events were observed during ebb and low tide, the majority of concentrations were below the
 473 EPA's threshold for safe public use, demonstrating that the observed conditions did not pose a
 474 public health hazard. Yet, the observed increase in ENT concentrations during ebb tide in a large
 475 and dynamic waterway like Taylor's Creek demonstrates that tidal floods and stormwater
 476 network inundation can serve as a source of fecal contamination to surface waters and are worthy

477 of further investigation as an emerging public health concern, particularly in coastal communities
 478 that drain to relatively small tidal creeks with minimal potential to flush or dilute pollutants.

479 **Table 1.** Linear regression models of baseline conditions (top) and perigean spring tide
 480 conditions (bottom) between log₁₀-transformed ENT concentrations (log₁₀ MPN) and tidal or
 481 rainfall factors.

<i>Baseline Conditions (n = 166 observations); random effect = sampling location</i>					
Explanatory Variables (fixed effect)	Conditional R ² (full model)	Marginal R ² (fixed effects)	p-value (alpha)	Coefficient	Standard Error
<i>Tidal Factors</i>					
Tidal Height	0.174	0.056	< 0.001	-0.15	0.03
Time to Last High Tide	0.159	0.037	< 0.001	0.12	0.03
Height of Last High Tide	0.124	0.009	0.073	-0.06	0.03
<i>Rainfall Factors</i>					
Prior 3-hour rainfall	0.231	0.105	< 0.001	0.21	0.03
Prior 6-hour rainfall	0.273	0.144	< 0.001	0.24	0.03
Prior 12-hour rainfall	0.385	0.268	< 0.001	0.34	0.03
Prior 24-hour rainfall	0.458	0.346	< 0.001	0.38	0.03
Prior 48-hour rainfall	0.395	0.313	< 0.001	0.36	0.03
Prior 72-hour rainfall	0.301	0.212	< 0.001	0.29	0.03
<i>Perigean Spring Tide Conditions (n = 89); random effects = sampling location, categorical tidal stage, flood</i>					
Explanatory Variables (fixed effect)	Conditional R ² (full model)	Marginal R ² (fixed effects)	p-value (alpha)	Coefficient	Standard Error
<i>Tidal Factors</i>					
Tidal Height	0.34	0.206	< 0.001	-0.28	0.07
Time to Last High Tide	0.348	0.134	0.041	0.22	0.11
Height of Last High Tide	0.394	0.006	0.212	-0.05	0.04
<i>Rainfall Factors</i>					
Prior 3-hour rainfall	0.415	0	0.775	-0.01	0.05

Prior 6-hour rainfall	0.373	0.003	0.516	0.03	0.05
Prior 12-hour rainfall	0.376	0.002	0.558	0.03	0.05

482 From the results of our robust linear mixed effect models for the perigean spring tides
483 (**Table 1**), tidal height at sample collection and time to last high tide were associated with the
484 greatest and second greatest marginal R^2 values (0.21 and 0.13, respectively). Though they
485 cannot explain the majority of ENT variance (i.e., they do not have marginal $R^2 > 0.5$), the
486 marginal R^2 values of tidal height at sample collection and time to last high tide support prior
487 recommendations by Price et al. (2021) that tidal variables be included and documented as part
488 of coastal ENT monitoring efforts, as tidal effects can play a role in transporting ENT within
489 coastal systems.

490 Height of the last high tide and rainfall variables had low marginal R^2 values for the
491 perigean spring tide conditions and coefficients that were not significantly different from zero
492 (**Table 1**). Because height of last high tide was not a significant descriptor of ENT concentration
493 variance, we conclude that maximum inundation prior to sampling was not the most important
494 factor explaining the elevated ENT concentrations during ebb tide for our study site. Regardless,
495 height of the last high tide should not be discounted as a potential variable to monitor, as our
496 observational period may not have captured high enough water level events to exhibit a
497 significant relationship with ENT concentration. Future SLR projections indicate more frequent
498 and greater inundation of stormwater networks, such that height of the last high tide may become
499 an important factor to explain elevated ENT concentrations as tidal water could reach sources of
500 fecal contamination further into the stormwater network. Additionally, since data collection
501 occurred in one municipality, other coastal stormwater network configurations may have
502 increases in ENT concentrations at tidal heights comparable to the tidal heights measured in this
503 study.

504 Likewise, our results should not indicate that rainfall is not an important descriptor to
505 ENT variability during the ebb tide and drainage of the stormwater network, as other studies
506 have demonstrated a direct link between rainfall and ENT concentration in coastal waterways
507 (Mallin et al., 2000). The low marginal R^2 values of our tested rainfall variables likely stem from
508 our sampling design, which targeted the tidal dynamics of the 6-7 hour period between the higher
509 high tide and the higher low tide, and did not include many rainfall events.

510 3.5 Stormwater runoff drives higher ENT concentrations than tidal inundation

511 During baseline conditions, stormwater runoff drove higher ENT concentrations in the
512 waterway than tidal inundation. Prior rainfall totals were significantly related to daily ENT
513 variance in the waterway during baseline conditions (Table 1). Specifically, antecedent rainfall
514 over 3, 6, 12, 24, 48, and 72 hours prior to sample collection had larger marginal R^2 values (0.10-
515 0.35) in the baseline model than the significant tidal variables (0.04-0.06). The marginal R^2
516 values were greatest for the 24-hour ($R^2 = 0.346$) and 48-hour rainfall models ($R^2 = 0.313$),
517 likely demonstrating lagged effects between rainfall and the accumulation of runoff over the
518 broader drainage area. Many studies have reported increased FIB concentrations in waterways
519 following rainfall events (Converse et al., 2011; Gonzalez et al., 2012; Parker et al., 2010;
520 Stumpf et al., 2010). However, while antecedent rainfall predominantly explained ENT

521 concentrations during baseline conditions (i.e., when there is no roadway flooding from complete
522 stormwater inundation by tides), rain variables did not significantly explain ENT variance during
523 perigeon spring tides, as discussed above.

524 Though rain variables were not significant descriptors of ENT variance during perigen
525 tides, we observed that recent rainfall events coincided with the maximum ENT concentrations
526 observed in Taylor's Creek during the perigeon spring tide periods (Fig 5). On July 15, 2022,
527 sample collection of the low tide samples coincided with a compound flood that was caused by
528 rainfall plus reduced capacity in the stormwater network due to tidal inundation. These samples
529 were collected 20 hours after a 22-mm, 8-hour rainfall event that occurred the previous day, and
530 during the first hour of a 17-mm rainstorm that lasted over 9 hours. Approximately 3.6 mm of
531 rainfall occurred during the first hour of the event. This compound flood event had the greatest
532 ENT concentrations observed in the waterway during both perigeon spring tides, indicating that
533 compound flood events have the potential to bring greater magnitudes of fecal contamination to
534 waterways compared to tidal inundation alone. Further research is needed to quantify the
535 relationship between rainfall depth, extent of tidal inundation, and the magnitude of fecal
536 contamination in the waterway, however our sampling of this one compound flood event
537 demonstrates the importance of how different flood types can cause varying amounts of fecal
538 contamination in coastal waterways.

539 **4 Conclusions**

540 Our findings indicate that chronic stormwater network inundation and tidal flooding
541 caused by SLR present pathways for fecal contamination of coastal surface waters, but research
542 is needed to fully understand whether network inundation and floods create public health
543 hazards. In this study, we consistently observed high ENT concentrations above the US EPA's
544 single sample maximum threshold for safe public use of recreational waters in tidal and
545 compound floodwaters on a roadway in Beaufort, NC, but did not observe similarly concerning
546 ENT concentrations in Taylor's Creek, the adjacent coastal waterway, as a function of tide-
547 driven stormwater network inundation. We observed minor floods with minimal overland
548 footprints, leading us to believe that the sources of the elevated ENT in the floodwaters were
549 within the stormwater network, and could include undrained stormwater runoff, pipe biofilms
550 and sediment, and exfiltrated sewage. Rainfall-driven runoff produced higher ENT
551 concentrations in Taylor's Creek than stormwater network inundation and tidal flooding,
552 reinforcing that stormwater runoff is the dominant driver of increased ENT concentrations in the
553 coastal waterway. However, we observed short-lived increases in ENT concentrations in
554 Taylor's Creek as perigeon spring tides receded from the stormwater network, and we
555 hypothesize the temporary increase in ENT concentrations is due to dilution or flushing given
556 that Taylor's Creek is a large coastal waterway. In relatively small tidal creeks draining urban
557 centers, the effects of dilution and flushing may not be as apparent, and the role of stormwater
558 network inundation and tidal flooding on ENT concentrations may be more pronounced.

559 This study provided needed longitudinal water quality observations across a two-month
560 period that included nine tidal floods from two perigeon spring tide events, which allowed us to
561 assess potential public health hazards from tidal flooding and make inferences on the relative
562 roles of stormwater network inundation, tidal flooding, and rain on fecal contamination both in a
563 coastal waterway and roadway floodwaters. However, the small size of the tidal floods we

564 observed prevents us from concluding whether more extensive floods are associated with higher
565 or lower ENT concentrations. Additionally, while our results demonstrate that tidal floods are
566 associated with problematic water quality impacts as was shown in previous studies (Macías-
567 Tapia et al., 2021, 2023; Hart et al., 2020; Price et al., 2021; McKenzie et al., 2021), similar
568 studies as the one presented here should be conducted across more locations to better understand
569 site-specific effects related to stormwater infrastructure and land use. We suggest that future
570 work incorporate sampling across multiple seasons, communities, and flood extents to better
571 understand the prevalence of poor water quality from chronic stormwater network inundation
572 and tidal flooding. Seasonal differences may contribute to the persistence of ENT within the
573 stormwater network, while community differences in infrastructure, topography, land use, and
574 waterway size could contribute to the type and number of ENT sources as well as the effect of
575 tidal flushing on ENT concentrations in the waterway.

576 Ultimately, the water quality effects of chronic stormwater network inundation and tidal
577 flooding are evolving given the non-stationarity of global climate change and SLR. SLR brings
578 uncertainty to whether tidally-driven inundation and associated pollutant loading will remain at
579 their current levels, as the magnitude of the loading will likely change with increased flooding
580 frequency and damage to infrastructure. For Beaufort and other cities on the Atlantic coast of the
581 US, rates of SLR are 30% higher than the global average of 3 mm/year (Ezer & Atkinson, 2014),
582 meaning that future repetition of this study could produce differing results as tidally-driven
583 inundation becomes more intense and widespread.

584 Acknowledgments

585 The authors report no financial conflicts of interest nor affiliations for any author that may be
586 perceived as having a conflict of interest with respect to the results of this paper. We thank David
587 Bennett and Grant Caraway of the North Carolina Maritime Museum for access to their dock,
588 and Dave Eggleston, Melissa LaCroce, and the NC State University Center for Marine Sciences
589 and Technology for use of lab facilities. This work was supported by the U.S. National Science
590 Foundation (NSF) award number 2047609 and the U.S. Geological Survey (USGS) Southeast
591 Climate Adaptation Science Center award G23AC00548 via a Global Change Fellowship to M.
592 Carr. This paper's contents are solely the responsibility of the authors and do not necessarily
593 represent the views of the Southeast Climate Adaptation Science Center, USGS, or NSF.

594 Open Research

595 All data and code are provided as supporting materials with the manuscript for peer review
596 purposes. Following acceptance, the data and code will be archived with Dryad.

597 References

- 598 Allen, T. R., Crawford, T., Montz, B., Whitehead, J., Lovelace, S., Hanks, A. D., Christensen, A.
599 R., & Kearney, G. D. (2019). Linking Water Infrastructure, Public Health, and Sea Level
600 Rise: Integrated Assessment of Flood Resilience in Coastal Cities. *Public Works
601 Management & Policy*, 24(1), 110–139. <https://doi.org/10.1177/1087724X18798380>
- 602 Befus, K. M., Kurnizki, A. P. D., Kroeger, K. D., Eagle, M. J., & Smith, T. P. (2023).

- 603 Forecasting Sea Level Rise-driven Inundation in Diked and Tidally Restricted Coastal
604 Lowlands. *Estuaries and Coasts*, 46(5), 1157–1169. [https://doi.org/10.1007/s12237-023-](https://doi.org/10.1007/s12237-023-01174-1)
605 01174-1
- 606 Boehm, A. B. (2007). Enterococci Concentrations in Diverse Coastal Environments Exhibit
607 Extreme Variability. *Environmental Science & Technology*, 41(24), 8227–8232.
608 <https://doi.org/10.1021/es071807v>
- 609 Burkhart, T. H. (Tsung H. S. (2013). *Biofilms as sources of fecal bacteria contamination in the*
610 *stormwater drainage system in Singapore* [Thesis, Massachusetts Institute of
611 Technology]. <https://dspace.mit.edu/handle/1721.1/82805>
- 612 Center for Operational Oceanographic Products and Services. (2022). Tide & Currents for
613 Beaufort, Duke Marine Lab, NC - Station ID: 8656483. National Oceanic and
614 Atmospheric Administration.
615 <https://tidesandcurrents.noaa.gov/stationhome.html?id=8656483>
- 616 Converse, R. R., Piehler, M. F., & Noble, R. T. (2011). Contrasts in concentrations and loads of
617 conventional and alternative indicators of fecal contamination in coastal stormwater.
618 *Water Research*, 45(16), 5229–5240. <https://doi.org/10.1016/j.watres.2011.07.029>
- 619 Division of Water Resources. (2023, March). *2022 North Carolina 303(d) List*. North Carolina
620 Department of Environmental Quality.
621 <https://edocs.deq.nc.gov/WaterResources/DocView.aspx?dbid=0&id=2738821>
- 622 Dangendorf, S., Hendricks, N., Sun, Q., Klinck, J., Ezer, T., Frederikse, T., ... & Törnqvist, T. E.
623 (2023). Acceleration of US Southeast and Gulf coast sea-level rise amplified by internal
624 climate variability. *Nature Communications*, 14(1), 1-11.
- 625 Ezer, T., & Atkinson, L. P. (2014). Accelerated flooding along the U.S. East Coast: On the
626 impact of sea-level rise, tides, storms, the Gulf Stream, and the North Atlantic
627 Oscillations. *Earth's Future*, 2(8), 362–382. <https://doi.org/10.1002/2014EF000252>
- 628 Gold, A., Anarde, K., Grimley, L., Neve, R., Srebnik, E. R., Thelen, T., Whipple, A., & Hino, M.
629 (2023). Data From the Drain: A Sensor Framework That Captures Multiple Drivers of
630 Chronic Coastal Floods. *Water Resources Research*, 59(4), e2022WR032392.
631 <https://doi.org/10.1029/2022WR032392>
- 632 Gold, A. C., Brown, C. M., Thompson, S. P., & Piehler, M. F. (2022). Inundation of Stormwater
633 Infrastructure Is Common and Increases Risk of Flooding in Coastal Urban Areas Along
634 the US Atlantic Coast. *Earth's Future*, 10(3), e2021EF002139.
635 <https://doi.org/10.1029/2021EF002139>
- 636 Gonzalez, R. A., Conn, K. E., Crosswell, J. R., & Noble, R. T. (2012). Application of empirical
637 predictive modeling using conventional and alternative fecal indicator bacteria in eastern
638 North Carolina waters. *Water Research*, 46(18), 5871–5882.
639 <https://doi.org/10.1016/j.watres.2012.07.050>
- 640 Habel, S., Fletcher, C. H., Anderson, T. R., & Thompson, P. R. (2020). Sea-Level Rise Induced

- 641 Multi-Mechanism Flooding and Contribution to Urban Infrastructure Failure. *Scientific*
642 *Reports*, 10, 3796. <https://doi.org/10.1038/s41598-020-60762-4>
- 643 Hart, J. D., Blackwood, A. D., & Noble, R. T. (2020). Examining coastal dynamics and
644 recreational water quality by quantifying multiple sewage specific markers in a North
645 Carolina estuary. *Science of The Total Environment*, 747, 141124.
646 <https://doi.org/10.1016/j.scitotenv.2020.141124>
- 647 Health and Ecological Criteria Division, Office of Science and Technology. (2012, December).
648 Recreational Water Quality Criteria. (EPA-820-F-12-061). Environmental Protection
649 Agency. Office of Water. [https://www.epa.gov/sites/default/files/2015-](https://www.epa.gov/sites/default/files/2015-10/documents/rwqc2012.pdf)
650 [10/documents/rwqc2012.pdf](https://www.epa.gov/sites/default/files/2015-10/documents/rwqc2012.pdf)
- 651 IDEXX. (2019, May). Standard Test Method for Enterococci in Water Using Enterolert. (ASTM
652 D6503-19). IDEXX. <https://www.astm.org/d6503-19.html>
- 653 Koller, M. (2016). robustlmm: An R Package for Robust Estimation of Linear Mixed-Effects
654 Models. *Journal of Statistical Software*, 75, 1–24. <https://doi.org/10.18637/jss.v075.i06>
- 655 Lewis, D. J., Atwill, E. R., Pereira, M. das G. C., & Bond, R. (2013). Spatial and Temporal
656 Dynamics of Fecal Coliform and Escherichia coli Associated with Suspended Solids and
657 Water within Five Northern California Estuaries. *Journal of Environmental Quality*,
658 42(1), 229–238. <https://doi.org/10.2134/jeq2011.0479>
- 659 Lüdecke, D., Ben-Shachar, M., Patil, I., & Makowski, D. (2020). Extracting, Computing and
660 Exploring the Parameters of Statistical Models using R. *Journal of Open Source*
661 *Software*, 5(53), 2445. <https://doi.org/10.21105/joss.02445>
- 662 Lüdecke, D., Ben-Shachar, M. S., Patil, I., Waggoner, P., & Makowski, D. (2021). performance:
663 An R Package for Assessment, Comparison and Testing of Statistical Models. *Journal of*
664 *Open Source Software*, 6(60), 3139. <https://doi.org/10.21105/joss.03139>
- 665 Macías-Tapia, A., Mulholland, M. R., Selden, C. R., Loftis, J. D., & Bernhardt, P. W. (2021).
666 Effects of tidal flooding on estuarine biogeochemistry: Quantifying flood-driven nitrogen
667 inputs in an urban, lower Chesapeake Bay sub-tributary. *Water Research*, 201, 117329.
668 <https://doi.org/10.1016/j.watres.2021.117329>
- 669 Macías-Tapia, A., Mulholland, M. R., Selden, C. R., Loftis, J. D., & Bernhardt, P. W. (2023).
670 Five Years Measuring the Muck: Evaluating Interannual Variability of Nutrient Loads
671 From Tidal Flooding. *Estuaries and Coasts*, 46(7), 1756–1776.
672 <https://doi.org/10.1007/s12237-023-01245-3>
- 673 Mallin, M. A., Williams, K. E., Esham, E. C., & Lowe, R. P. (2000). Effect of Human
674 Development on Bacteriological Water Quality in Coastal Watersheds. *Ecological*
675 *Applications*, 10(4), 1047–1056. [https://doi.org/10.1890/1051-](https://doi.org/10.1890/1051-0761(2000)010[1047:EOHDOB]2.0.CO;2)
676 [0761\(2000\)010\[1047:EOHDOB\]2.0.CO;2](https://doi.org/10.1890/1051-0761(2000)010[1047:EOHDOB]2.0.CO;2)
- 677 McKenzie, T., Habel, S., & Dulai, H. (2021). Sea-level rise drives wastewater leakage to coastal
678 waters and storm drains. *Limnology and Oceanography Letters*, 6(3), 154–163.

- 679 <https://doi.org/10.1002/lo12.10186>
- 680 National Oceanic and Atmospheric Administration. (2022). Northern Hemisphere Moon Phases
681 for 2022. Tides and Currents - Astronomical Data.
682 https://tidesandcurrents.noaa.gov/moon_phases.shtml?year=2022
- 683 Olds, H. T., Corsi, S. R., Dila, D. K., Halmo, K. M., Bootsma, M. J., & McLellan, S. L. (2018).
684 High levels of sewage contamination released from urban areas after storm events: A
685 quantitative survey with sewage specific bacterial indicators. *PLoS Medicine*, *15*(7),
686 e1002614. <https://doi.org/10.1371/journal.pmed.1002614>
- 687 Parker, J. K., McIntyre, D., & Noble, R. T. (2010). Characterizing fecal contamination in
688 stormwater runoff in coastal North Carolina, USA. *Water Research*, *44*(14), 4186–4194.
689 <https://doi.org/10.1016/j.watres.2010.05.018>
- 690 Price, M. T., Blackwood, A. D., & Noble, R. T. (2021). Integrating culture and molecular
691 quantification of microbial contaminants into a predictive modeling framework in a low-
692 lying, tidally-influenced coastal watershed. *Science of The Total Environment*, *792*,
693 148232. <https://doi.org/10.1016/j.scitotenv.2021.148232>
- 694 R Core Team (2013). R: A language and environment for statistical computing. R Foundation for
695 Statistical Computing, Vienna, Austria. ISBN 3-900051-07-0, URL [http://www.R-](http://www.R-project.org/)
696 [project.org/](http://www.R-project.org/)
- 697 Sercu, B., Van De Werfhorst, L. C., Murray, J. L., & Holden, P. A. (2011). Sewage exfiltration
698 as a source of storm drain contamination during dry weather in urban watersheds.
699 *Environmental science & technology*, *45*(17), 7151-7157.
- 700 State Climate Office of North Carolina. (2022) *Michael J Smith Field Airport (KMRH) hourly*
701 *and daily rainfall, June-August 2022* [Data set]. NOAA National Weather Service.
702 <https://products.climate.ncsu.edu/data/>
- 703 Strauss, B. H., Ziemiński, R., Weiss, J. L., & Overpeck, J. T. (2012). Tidally adjusted estimates
704 of topographic vulnerability to sea level rise and flooding for the contiguous United
705 States. *Environmental Research Letters*, *7*(1), 014033. [https://doi.org/10.1088/1748-](https://doi.org/10.1088/1748-9326/7/1/014033)
706 [9326/7/1/014033](https://doi.org/10.1088/1748-9326/7/1/014033)
- 707 Stumpf, C. H., Piehler, M. F., Thompson, S., & Noble, R. T. (2010). Loading of fecal indicator
708 bacteria in North Carolina tidal creek headwaters: Hydrographic patterns and terrestrial
709 runoff relationships. *Water Research*, *44*(16), 4704–4715.
710 <https://doi.org/10.1016/j.watres.2010.07.004>
- 711 Sweet, W., Hamlington, B.D., Kopp, R. E., & Zuzak, C. (2022). *Global and Regional Sea Level*
712 *Rise Scenarios for the United States: Updated Mean Projections and Extreme Water*
713 *Level Probabilities Along U.S. Coastlines* (p. 111) [Technical Report]. National Oceanic
714 and Atmospheric Administration.
715 [https://aambpublicoceanservice.blob.core.windows.net/oceanserviceprod/hazards/sealeve](https://aambpublicoceanservice.blob.core.windows.net/oceanserviceprod/hazards/sealevelrise/noaa-nos-techrpt01-global-regional-SLR-scenarios-US.pdf)
716 [lrise/noaa-nos-techrpt01-global-regional-SLR-scenarios-US.pdf](https://aambpublicoceanservice.blob.core.windows.net/oceanserviceprod/hazards/sealevelrise/noaa-nos-techrpt01-global-regional-SLR-scenarios-US.pdf)

- 717 University of North Carolina - Chapel Hill. (2022). *2022 King Tides Calendar*. North Carolina
718 King Tides Project. <https://nckingtides.web.unc.edu/>
- 719 Wade, T.J., Pai, N., Joseph N.S. Eisenberg, & Colford, J.M. (2003). Do U.S. Environmental
720 Protection Agency Water Quality Guidelines for Recreational Waters Prevent
721 Gastrointestinal Illness? A Systematic Review and Meta-Analysis. *Environmental Health*
722 *Perspectives*, *111*(8): 1102–1109.